Ancient high Pt/Os crustal contaminants can explain radiogenic 186Os in intraplate magmas

DOI:
10.1016/j.epsl.2019.04.039

Document Version
Accepted author manuscript

Ancient high Pt/Os crustal contaminants can explain radiogenic ^{186}Os in intraplate magmas

James M.D. Day[1], Brian O'Driscoll[2]

[1]Scripps Institution of Oceanography, La Jolla, CA 92093, USA

[2]Department of Earth and Environmental Sciences, University of Manchester, MI3 9PL, UK

For submission to: ***Earth and Planetary Science Letters***

Abstract length: 335

Total length: 4566

References: 49

Figures: 6

Tables: 1 (and a *Supplementary Table*)

Keywords: Chromitites; layered intrusions; crust; deep mantle; platinum-osmium; rhenium-osmium

Abstract

The origin of variations in $^{186}Os/^{188}Os$ ratios amongst mantle-derived basaltic and komatiitic lavas remains controversial, with opposing models arguing for deep core-mantle versus shallow mantle sources. Crustal contamination has generally not been favoured due to the low Os contents of such sources, meaning that variations in $^{186}Os/^{188}Os$ would require involvement of extremely high proportions of crustal material. Here we re-examine crustal contamination as an effective means for generating significant $^{186}Os/^{188}Os$ variations in Earth materials. Using chromitites and peridotites from the Stillwater, Muskox and Rum layered intrusions, we show that radiogenic $^{186}Os/^{188}Os$ ratios are correlated with $^{187}Os/^{188}Os$ ratios and can only be explained by shallow-level mixing processes and crustal contamination. The samples have $\delta^{186}Os$ ($[\{(^{186}Os/^{188}Os_{sample[t]}/^{186}Os/^{188}Os_{PM(t)}) -1\} \times 1000]$, where the modern primitive mantle [PM] $^{186}Os/^{188}Os$ is 0.1198388) values ranging between 0.04 to 0.15 for the ~2.7 Ga Stillwater Igneous Complex, -0.05 to 0.17 for the ~1.27 Ga Muskox Intrusion, and 0.02 to 0.13 for the ~0.06 Ga Rum Layered Suite. The highly siderophile element (HSE: Os, Ir, Ru, Pt, Pd, Re) contents of the chromitites and peridotites can be modelled through high sulfide-melt partitioning (typically >8000) and emphasise the role of S-saturation and HSE scavenging. Considering the high sulfide-melt partitioning and accounting for high silicate melt to sulfide melt ratios (R-factor), it is possible to explain the variations in ^{186}Os-^{187}Os in layered intrusions using calculated Os isotope crustal evolution growth models. These calculations indicate that <4% of ancient high Pt/Os crustal contributions can explain the composition of the chromitites and peridotites that were examined. Our observations are consistent with published models for chromitite genesis that invoke either crustal melt-primitive melt mixing, or cumulate assimilation. A crustal origin for radiogenic ^{186}Os is a possible cause for $^{186}Os/^{188}Os$ ratio variations observed in some komatiites. It is more difficult to explain radiogenic $^{186}Os/^{188}Os$ measured in Hawaiian lavas by crustal contamination processes. Instead, ancient high Pt/Os oceanic crust, shallow mantle sources such as metasomatic sulfide, or metal-rich large low-shear wave velocity provinces at the core-mantle boundary, all remain valid explanations.

1. Introduction

The long-lived ^{190}Pt-^{186}Os chronometer (470 Ga half-life, $\lambda = 1.54 \times 10^{-12}$ y^{-1}; Walker et al., 1997) has been considered as a potential tracer of outer core contributions to deeply-sourced mantle plumes (Walker et al., 1997; Brandon et al., 1998; 1999; 2003). High-precision ^{186}Os-^{187}Os studies have shown that radiogenic $^{186}Os/^{188}Os$ ratios occur in some Hawaiian ocean island basalts (OIB), as well as Archean komatiites, but are not pervasive features of intraplate magmatism (Puchtel et al., 2005; Brandon et al., 2007; Ireland et al., 2011). The concept that early inner core crystallization (with preferential incorporation of Os into early-crystalizing phases) would lead to high Pt/Os in the outer liquid core that would then contribute to mantle plumes, has become increasingly untenable. This is mainly due to the young inferred age of the inner core of ≤2.5 Ga, and likely between 0.7-1.5 Ga (Labrosse et al., 2001; Lassiter, 2006; Nimmo, 2007; Biggin et al., 2015). Derivation of radiogenic ^{186}Os from deep long-lived high-Pt/Os reservoirs represented by geophysically-detected 'large low-shear-velocity provinces' (LLSVPs) at the core-mantle boundary (Humayun, 2011) remains to be fully tested, with shallow long-lived Pt/Os reservoirs also being suggested to cause ^{186}Os enrichment in some lavas (e.g., Smith, 2003; Baker & Jensen, 2004; Lassiter, 2006; Luguet et al., 2008).

The likely sources of radiogenic $^{186}Os/^{188}Os$ are restricted by the fact that ^{190}Pt makes up only 0.01292% of natural Pt, and is an extremely long-lived unstable isotope, so a radiogenic ^{186}Os component must have the characteristics of both being extremely old (>1 Ga) and having high time-integrated Pt/Os. A compounding issue is that peridotites and mantle-derived melts typically have relatively high Os (≥1 ppb), compared to sources with high Pt/Os, like continental crust, which only has 0.031 ppb Os (Peucker-Enrinbrink & Jahn, 2001; Day, 2013). Sources of high time-integrated Pt/Os have been suggested to include metasomatic sulfides and pyroxenites with high Os contents (e.g., Luguet et al., 2008; O'Driscoll et al. 2015). It is possible that crust with high time-integrated Pt/Os can generate radiogenic ^{186}Os in some intraplate magmas. This is due to Pt and Os both being highly siderophile elements (HSE: Os, Ir, Ru, Pt, Rh, Pd, Re, Au) that are also high chalcophile. It has been demonstrated that sulfide fractionation in S-saturated melts can lead to effective scavenging of the HSE, with very high sulfide-melt partitioning (D >100,000; Mungall & Brenan, 2014). These high D values coupled with the mass ratio of silicate magma available to equilibrate with sulfide liquid (R; Campbell & Naldrett, 1979):

$$\text{Sulfide liquid content} = (\text{HSE}_{\text{content of silicate magma}} \times D[R+1]))/(R+D)$$

can lead to significant enrichment from otherwise low HSE sources.

The so-called 'R-factor' models have been applied to layered intrusions with considerable success to explain enrichment of the HSE and associated mineralization (e.g., Barnes & Ripley, 2016). These models, when coupled with Os isotopes and other tracers of crustal contributions, have revealed significant crustal contributions of both S and the HSE to mantle-derived magmas (e.g., Day et al., 2008; O'Driscoll et al., 2009). These observations raise the possibility that scavenging of the HSE by sulfide can lead to enhanced crustal contributions to intraplate magmas and, correspondingly to potential enrichments in both ^{187}Os and ^{186}Os from high time-integrated Re/Os and Pt/Os sources. In this contribution, we demonstrate the importance of this process for chromitite seams from layered intrusions of differing ages (2.7 Ga Stillwater Igneous Complex; 1.27 Ga Muskox Intrusion; 0.060 Ga Rum Igneous Complex) and discuss how it may be important in other intraplate magmatic settings.

2. Methods

Osmium isotope and highly siderophile element (HSE; Os, Ir, Ru, Pt, Pd, Re) abundance analyses were performed at the *Scripps Isotope Geochemistry Laboratory*. Bulk rock samples were ground to fine powders. In the case of Muskox chromitites, two separate powders were made for each seam. An appropriate amount of powder to obtain 100 ng total Os was precisely weighed into cleaned Pyrex Carius tubes and sealed with 7 mL of multiply Teflon distilled (TD) 15.7M HNO_3 purged of Os by repeated treatment with H_2O_2, and 4 mL of TD 12M HCl. The Carius tubes were shaken, placed into a convection oven and then heated for 72 hrs at 270°C. After cooling, the Carius tubes were broken and solutions were completely liberated and placed in new pre-cleaned Teflon vials where they were precisely weighed. An aliquot representing 5% of the total mass was removed and used to obtain isotope dilution HSE (Os, Ir, Ru, Pt, Pd, Re) abundance data and ^{187}Re/^{188}Os and ^{190}Pt/^{188}Os ratios. Carbon tetrachloride (CCl_4) was added to the remaining 95% HNO_3/HCl solution to extract Os. A total of four CCl_4 extractions were performed to remove Os, with the CCl_4 being equilibrated with triple Teflon distilled 9M HBr.

This mixture was left overnight, after which the CCl_4 was removed and the HBr was dried down. Three micro-distillations were then performed for each sample using H_2SO_4-$Cr_2O^{2-}_7$ as the oxidizer and TD 9M HBr as the distillate (Day et al., 2017).

High-precision Os isotope data were obtained by negative thermal ionization mass spectrometry (N-TIMS) using a *ThermoScientific* Triton, with a high purity O_2 bleed at a constant source pressure of 1 $\times 10^{-7}$ mbar. Data were collected in static mode using Faraday collectors with signal intensities of >100 mV on mass 234 ($^{186}Os^{16}O_3^-$), generated for >360 ratios (17s integration time per ratio, 30 s baselines measured every 20 ratios), with the goal of obtaining an in-run precision of ±-25 ppm (2 Sigma Error), or better, for $^{186}Os/^{188}Os$ on 75 ng Os loads. We used a $^{17}O/^{16}O$ composition of 0.0003749 and $^{18}O/^{16}O$ of 0.0020439, identical to that of Day et al. (2017). Following O corrections, an instrumental mass fractionation correction was applied using the exponential law and a $^{192}Os/^{188}Os$ ratio of 3.083. Potential interferences were monitored during runs at masses 230 ($^{198}Pt^{16}O_2^-$), 231 ($^{183}W^{16}O_3^-$) and 233 ($^{185}Re^{16}O_3^-$); these had no measurable effects on Os isotopic compositions. During the analytical campaign, 12 separate 75 ng Os loads of the Johnson Matthey Os internal standard (UMCP) yielded an average $^{186}Os/^{188}Os$ of 0.1198460 ±13 (2 SD) and $^{187}Os/^{188}Os$ of 0.1137950 ±23 (2 SD). These values agree well with previously reported measurements for mantle rocks by Brandon et al. (2000; 2006) and Day et al. (2017). As an independent measure of analytical reproducibility, we measured the OSUM8 standard ($^{186}Os/^{188}Os$ = 0.1198383 ±13 and $^{187}Os/^{188}Os$ = 0.1314654 ±27; n = 12), obtaining values within error of previously reported values ($^{186}Os/^{188}Os$ = 0.1198390 ±5 and $^{187}Os/^{188}Os$ = 0.1314615 ±23; n = 30; Day et al., 2017). As suggested by Day et al. (2017), we normalized samples in this study to their nominal UMCP values ($^{186}Os/^{188}Os$ = 0.1198458; $^{187}Os/^{188}Os$ = 0.1137852).

For HSE abundance data, the 5% aliquots were digested in sealed borosilicate Carius tubes with isotopically enriched multi-element spikes (^{99}Ru, ^{106}Pd, ^{185}Re, ^{190}Os, ^{191}Ir, ^{194}Pt), 7 mL of a 1:2 mixture of TD 12M HCl and purged TD 15.7M HNO_3. Samples were digested to a maximum temperature of 270˚C in an oven for 72 hours. Osmium was triply extracted from the acid using CCl_4 and then back-extracted into HBr, prior to triple purification by micro-

distillation, and Re and the other HSE were recovered and purified from the residual solutions using standard anion exchange separation techniques (Day et al., 2016). Isotopic compositions and abundances of Os were measured in negative-ion mode using the *Triton*, and Re, Pd, Pt, Ru and Ir were measured using a *Cetac Aridus II* desolvating nebuliser coupled to a *ThermoScientific* iCAP Qc ICP-MS. Offline corrections for Os involved an oxide correction, an iterative fractionation correction using $^{192}Os/^{188}Os = 3.08271$, a ^{190}Os spike subtraction, and finally, an Os blank subtraction. Precision for $^{187}Os/^{188}Os$, determined by repeated measurement of the UMCP Johnson-Matthey standard, was better than ±0.2% (2 SD; 0.11379 ±11; $n = 5$). Rhenium, Ir, Pt, Pd and Ru isotopic ratios for sample solutions were corrected for mass fractionation using the deviation of the standard average run on the day over the natural ratio for the element. External reproducibility on HSE analyses was better than 0.5% for 0.5 ppb solutions. Total procedural blanks ($n = 2$) run with samples had $^{187}Os/^{188}Os = 0.42 \pm 0.02$, with quantities (in picograms) of 1.8 to 2.2 [Re], 8 to 16 [Pd], 2.7 to 3.2 [Pt], 9.9 to 11 [Ru], 0.6 to 1.4 [Ir] and 0.07 to 0.2 [Os]. All samples are blank corrected, with blanks representing <1% of the total analyte.

3. Results

Chromitite seams from the Stillwater, Muskox and Rum layered intrusions were targeted for their Os isotope and HSE abundance systematics (*Supplementary Table 1*), together with a native-iron bearing basalt lava from Disko Island, West Greenland, described previously (Pernet-Fisher et al., 2017). Chromitite from the Stillwater, Muskox and Rum layered intrusions have similar relative and absolute abundances of Os, Ir, Ru and Re (13-148 ppb Os, 16-156 ppb Ir, 49-300 ppb Ru, 0.04-2.5 ppb Re), resulting in a restricted range in Re/Os (0.052 ±0.065), Ir/Os (5.0 ±3.5) and Ru/Os ratios (1.39 ±0.76) (**Table 1; Figure 1**). The chromitites show more extreme ranges in Pd and Pt contents, with the Stillwater chromitites having relatively low abundances of these elements (94-200 ppb Pd, 2-16 ppb Pt) and low Pt/Os (0.025-0.24) and Pd/Os (1.2-2.9) ratios relative to Muskox (1065-4100 ppb Pd; 377-597 ppb Pt; Pt/Os = 8.8-36.8; Pd/Os = 21-304) or Rum (322-1312 ppb Pd, 226-1525 ppb Pt, Pt/Os = 2.6-19; Pd/Os = 0.9-22) chromitites. Rhenium and Os contents of the Muskox and Stillwater chromitites are within the ranges of previously reported data (Marcantonio et al., 1993; Lambert et al., 1994; Horan et al., 2001; Day et al., 2008). The Rum Unit 12 peridotite has a similar HSE pattern and concentrations to the

Unit 7/8 and Unit 11/12 chromitites, but the Unit 8 peridotite has relatively low Pt and Pd, and a broadly flat primitive-mantle normalized HSE pattern, in agreement with previous data (O'Driscoll et al., 2009). The Fe-bearing West Greenland Picrite analyzed in this study has an identical pattern to that previously obtained by Pernet-Fisher et al. (2017), with a positive Pt abundance anomaly.

High-precision $^{187}Os/^{188}Os$ measurements for chromitites from the Stillwater G and H seams (0.11547-0.11834; γ^{187}_{Os} = 4-7.4, where [γ^{187}_{Os} = ([$^{187}Os/^{188}Os_{sample(t)}/^{187}Os/^{188}Os_{PM(t)}$] -1) × 100], with PM being the primitive mantle composition), Muskox chromitites (0.13217-0.16899; γ^{187}_{Os} = 8.4-26.6), and Rum chromitites and peridotites (0.13464-0.13703; γ^{187}_{Os} = 4.2-5.9) are within the range of previously reported values for these units (Lambert et al., 1994; Day et al., 2008; O'Driscoll et al., 2009) (**Figure 2**). The measured $^{187}Os/^{188}Os$ ratio (0.1636; γ^{187}_{Os} = 23) for the Fe-bearing West Greenland picrite is more radiogenic than previously reported ratios (0.150-0.155), probably reflecting initial isotopic heterogeneity in the sample, as noted previously (Pernet-Fisher et al., 2017). The Fe-bearing West Greenland picrite yields the least radiogenic $^{186}Os/^{188}Os$ ratio (0.119832; $\delta^{186}Os$ = -0.06, where [δ^{186}_{Os} = ([$^{186}Os/^{188}Os_{sample(t)}/^{186}Os/^{188}Os_{PM(t)}$] -1) × 1000]), with Stillwater (0.119838-0.119850; $\delta^{186}Os$ = 0.04-0.15) and Rum (0.119842-0.119856; $\delta^{186}Os$ = 0.02-0.13) lying intermediate between this value and the generally more radiogenic Muskox chromitites (0.119847-0.119924; $\delta^{186}Os$ = -0.05-0.17) (**Table 1**).

4. Discussion

4.1 Chromitite formation and sulfide fractionation effects

Chromitite seams from the Stillwater, Muskox and Rum igneous complexes have similar absolute abundances of Os, Ir, Ru and Re, but more variable Pt and Pd. The compositions of the parental melts that fed the Muskox and Rum intrusions are preserved as the Keel dike (Muskox; Day et al., 2008) and as cross-cutting picrite dikes (Rum; Upton et al., 2002). The Muskox and Rum dikes have similar HSE abundances (in ppb: Keel dike = ~1.9 Os, ~1.6 Ir, ~6 Ru, ~10 Pt, ~2.5 Pd, ~0.4 Re [Day et al., 2008]; Rum M9 picrite dike = ~2.5 Os, ~0.9 Ir, ~2.9 Ru, ~3.5 Pt,

208 ~5.3 Pd, ~0.8 Re [O'Driscoll et al., 2009]). A comparison of the two dikes versus the chromitites
209 from their respective intrusions provides HSE enrichment factor estimates for chromitite
210 formation, which range from as low as a factor of 2-3 for Re, to ~16-95 times for Or, Ir and Ru
211 and from 50 to 965 for Pt and Pd (**Figure 3**). While this form of exercise cannot be performed
212 for Stillwater, where no primary melt HSE composition has been defined, the similarity in its
213 chromitite Os, Ir and Ru contents might suggest a similar enrichment factor during chromitite
214 petrogenesis.

215

216 The cause of HSE enrichment in stratiform mineralized zones in layered intrusions is
217 generally attributed to scavenging of these elements within sulfide and alloy phases. The HSE
218 are both siderophile and chalcophile with extremely high partition coefficients between sulfide
219 melt and silicate melt of 10^3 to 10^6 (Mungall & Brenan 2014). The consequence of this
220 behaviour is that sulfide-rich sidewall deposits and some sulfide-rich stratiform deposits can
221 become extremely enriched in the HSE (e.g., Barnes & Ripley, 2016), including economically
222 significant resources such as the Merensky Reef of the Bushveld Igneous Complex and the J-M
223 Reef of the Stillwater Igneous Complex.

224

225 To explore sulfide fractionation effects, we present models of sulfide-melt partitioning using
226 experimental values from Mungall & Brenan (2014) and empirical sulfide-melt partitioning
227 values from Chazey & Neal (2005) for the Muskox chromitites/Keel dike and the Rum
228 chromitites/M9 picrite dike (**Figure 3**). The experimentally determined sulfide-melt partitioning
229 from Mungall & Brenan (2014) is too high for Pd, Pt, Ru, Ir and Os to adequately explain the
230 HSE enrichments in either the Muskox or Rum chromitites. Conversely, the Chazey & Neal
231 (2005) values reproduce the Rum pattern well, but not the absolute enrichment factors. A best-fit
232 model to obtain the average enrichments of the HSE in the Muskox and Rum intrusions are
233 around 500 for Re, 8000 for Os and Ru, 16,000 for Ir, 25,000 for Pd and 30,000 for Pt. The low
234 Pt observed in the Stillwater chromitites suggest a low sulfide-melt partitioning for Pt for that
235 intrusion of ~2000. These model emphasise that sulfide-melt partitioning was broadly similar for
236 the HSE in chromitite seams for the Stillwater, Muskox and Rum layered igneous complexes.

4.2 Platinum-Os isotope evolution of mantle and crustal reservoirs

The most precise determinations of the long-term ^{187}Re-^{187}Os evolution of mantle and crustal reservoirs have revealed high $^{187}Re/^{188}Os$ (34.5), radiogenic average upper crust ($^{187}Os/^{188}Os$ = 1.4; Peucker-Ehrinbrink & Jahn, 2001) and a primitive mantle (analogous to bulk silicate Earth; BSE) composition ($^{187}Re/^{188}Os$ = 0.4253; $^{187}Os/^{188}Os$ = 0.1296 ±8; Meisel et al., 2001) that is only marginally more radiogenic than ordinary or enstatite chondrite groups (Ordinary chondrites $^{187}Re/^{188}Os$ = 0.4179; $^{187}Os/^{188}Os$ = 0.1280 ±8; Enstatite chondrites $^{187}Re/^{188}Os$ = 0.4206; $^{187}Os/^{188}Os$ = 0.1284 ±20; Carbonaceous chondrites $^{187}Re/^{188}Os$ = 0.3827; $^{187}Os/^{188}Os$ = 0.1258 ±16; Day et al., 2016). Correspondingly, the average $^{187}Os/^{188}Os$ value of the depleted upper mid-ocean ridge basalt mantle (DMM), based on abyssal peridotites is 0.1247 ± 0.0075 (Lassiter et al., 2014; Day et al., 2017), and is consistent with continental crust extraction to form a rhenium-depleted upper mantle through time.

Due to their typically very low Os contents, it is much harder to directly measure $^{186}Os/^{188}Os$ variations at high precision in continental crustal materials. Instead, we infer the gross crustal evolution curve from the difference between the depleted mantle $^{186}Os/^{188}Os$ (0.1198356 ±21) and BSE $^{186}Os/^{188}Os$ estimates (0.1198388 ±29; Day et al., 2017) to calculate the long-term Pt/Os ratio of the bulk crust (**Figure 4**). From these calculations, a $^{190}Pt/^{186}Os$ ratio of 0.00568 is obtained, and $^{186}Os/^{188}Os$ of 0.119856 averaged over 4.5 Ga. These values are lower than those estimated for the upper continental crust ($^{190}Pt/^{186}Os$ = 0.0176, $^{186}Os/^{188}Os$ = 0.119885), from loess assuming an average crustal age of 2.2 Ga (Peucker-Ehrinbrink & Jahn, 2001). These differences reflect the average compositional variation between crustal and mantle reservoirs assuming 4.5 Ga of differentiation versus the specific evolution of upper continental crustal reservoirs. In both cases the inference is that continental crustal reservoirs, while poor in Os (31 ppt in the upper crust), are radiogenic with respect to $^{186}Os/^{188}Os$, on average by up to 0.4‰ (or 400 ppm) for $\delta^{186}Os$. Chromitites seams from the Rum, Muskox and Stillwater intrusions and Noril'sk (Russia) sulfides all have more radiogenic $^{186}Os/^{188}Os$ compositions, on average, than BSE or DMM values, lying between these values and inferred crustal compositions. We explore the reasons for these compositions in *Section 4.4*, but first consider the unusual $^{186}Os/^{188}Os$

composition inferred for the Bushveld Igneous Complex (South Africa), which is a clear outlier in **Figure 4**.

4.3 The Bushveld Igneous Complex

Prior work to examine $^{186}Os/^{188}Os$ variations in layered intrusions at high-precision has been restricted to the study of sulfide ores from the ~250 Ma Noril'sk intrusions using negative thermal ionization mass spectrometry (N-TIMS; Walker et al., 1997), and the study of grains of laurite, cooperite, laurite-platarsite, sperrylite and Pt-Fe alloys from the Merensky Reef of the ~2050 Ma Bushveld Igneous Complex using laser ablation multi-collector inductively coupled plasma mass spectrometry (LA-MC-ICP-MS) (Coggan et al., 2011). While the study of Noril'sk ores yielded a relatively radiogenic initial $^{186}Os/^{188}Os$ composition and was also used to empirically derive the Pt-decay constant, the Merensky Reef study revealed a composite isochron age of 1995 ±50 Ma and an unradiogenic initial $^{186}Os/^{188}Os$ of 0.119819 ±6 (Coggan et al., 2011). This initial $^{186}Os/^{188}Os$ ratio for the Merensky Reef lies close to or below (within uncertainty) the Solar System Initial value estimated from chondrite meteorites (0.119823 ±5; Day et al., 2016b) or IIIAB iron meteorites (0.119824 ±9; Cook et al., 2004), and is significantly lower than the primitive mantle or chondritic values for $^{186}Os/^{188}Os$ estimated at 2.05 Ga (0.119832 ±5) (**Figure 4**). For the measurement of Merensky grains, Coggan et al. (2011) directly ablated materials into the carrier gas and Ar plasma, with measurement of potential interferences and offline interference corrections, including correction of a direct interference from ^{186}W using ^{182}W. Any over-correction on ^{186}Os for a potential ^{186}W interference would result in underreporting of the $^{186}Os/^{188}Os$ ratio. Given the very low initial $^{186}Os/^{188}Os$ value for the Merensky Reef reported by Coggan et al. (2011), and the clear distinctiveness of Bushveld data compared with the other layered intrusion data, we do not consider the available Bushveld data further in this discussion. High-precision N-TIMS analyses of Bushveld Igneous Complex chromitites and Merenksy Reef materials would be valuable for establishing the ^{186}Os-^{187}Os systematics of the world's largest layered igneous complex.

4.4 Crustal contamination and radiogenic ^{186}Os

Studies of $^{187}Os/^{188}Os$ ratios in layered intrusions have primarily attributed the large isotopic

297 variations to variable contributions from high time-integrated Re/Os crustal contaminants. A
298 compilation of layered intrusion initial $^{187}Os/^{188}Os$ ratios reveals significant crustal additions to
299 locations including Sudbury, Duluth, Voisey's Bay and Conowarra (Day et al., 2008). Crustal
300 contamination of lithologies in the Stillwater, Muskox and Rum intrusions have all been
301 demonstrated using Re-Os isotope systematics, typically in the range of 2 to 5 wt.% additions to
302 mantle-derived melts (Marcantonio et al., 1993; Lambert et al., 1994; Horan et al., 2001; Day et
303 al., 2008; O'Driscoll et al., 2009). The chromitite and peridotite samples measured all have
304 $^{187}Os/^{188}Os$ consistent with variable crustal contributions. For example, the Unit 8 peridotite and
305 associated Unit 7/8 chromitite are marginally less radiogenic than their Unit 11/12 equivalents in
306 the Rum intrusion, plausibly consistent with increasing crustal contamination between the two
307 units (O'Driscoll et al., 2009). Likewise, the Muskox Intrusion chromitites that we studied have
308 variable $^{187}Os/^{188}Os$ ratios, consistent with changing contributions from crustal sources in the
309 same cyclic unit (Day et al., 2008). It is more difficult to see systematic variation in the
310 Stillwater chromitites, but it is well-established that chromitites lower in the ultramafic series of
311 this intrusion show greater ranges in $^{187}Os/^{188}Os$ and putatively higher degrees of crustal
312 contamination than in the upper chromitites (Horan et al., 2001). Logic suggests that if variations
313 in $^{187}Os/^{188}Os$ originate from crustal contamination, then accompanying $^{186}Os/^{188}Os$ variations
314 were similarly generated, in this case by mingling of mantle-derived melts with high time-
315 integrated Pt/Os crust.
316
317 All three of the studied layered intrusions reside wholly or partly within relatively ancient
318 crust. The Stillwater Complex intruded Archean gneisses that yield ages >3.2 Ga (Boudreau,
319 2016). The Muskox intrusion was emplaced at the boundary between ~1.66 Ga sandstones of the
320 Hornby Bay Formation and the >1.8 Ga Wopmay paragneiss (Day et al., 2008), and the Rum
321 intrusion was emplaced at the unconformable contact between Archean-to-Paleoproterozoic
322 (Lewisian Complex) quartzofeldspathic gneisses and amphibolites and Neoproterozoic arkosic
323 sedimentary rocks of the (~1 Ga) Torridon Supergroup. A few of these rock-types have been
324 directly measured and have Pt/Os between 12 and 70 (Day et al., 2008). The overall evolution of
325 crustal sources would lead to radiogenic $^{186}Os/^{188}Os$ based on our calculations (*Section 4.3*), and
326 high Pt/Os basaltic and granitic crust are evident from the fractionation of compatible Os from
327 less compatible Pt during sulfide-fractionation processes (e.g., Day et al., 2013). The expectation

328 is therefore that crustal rocks have systematically high Pt/Os, and evolved with radiogenic
329 $^{186}Os/^{188}Os$, as also shown by Peucker-Ehrinbrink & Jahn (2001).
330
331 To examine the role of crustal contamination on mantle melt $^{186}Os/^{188}Os$ ratios we apply two
332 component R-factor mixing models between (type-1) a primitive mantle-like melt composition
333 ($\gamma^{187}Os = 0$, $\delta^{186}Os = 0 \pm 0.05$) and (type-2) a modified melt composition ($\gamma^{187}Os = 5$, $\delta^{186}Os = -$
334 0.05) and calculated crustal sources after fractional crystallization and sulfide fractionation
335 (**Figure 5**). The choice of the two compositions reflects the possibility that some layered
336 intrusions were replenished by mantle-derived melts that experienced limited prior crustal
337 contamination, whereas others were fed from staging reservoirs in the deeper crust. The models
338 assume that melts coming into the magma reservoir are either uncontaminated (type-1), or partly
339 contaminated (type-2) and then interact with crustal melts generated by partial fusion with
340 surrounding country rocks. Sulfide melt-silicate melt segregation occurs in these models due to
341 S-saturation, either from fractional crystallization and/or from assimilation of crustal S. The
342 result is a high R-factor, which is consistent with the requirement for high melt-rock ratios to
343 provide the Cr in forming the chromitites. Also shown in **Figure 5** are two-component mixing
344 models between the type-2 melt composition and potential Muskox Intrusion contaminants (i.e.,
345 Hornby Bay sandstone, Wopmay paragneiss).
346
347 The models in **Figure 5** reveal that simple two component mixing cannot account for the
348 radiogenic $^{186}Os/^{188}Os$ measured in the chromitites and peridotites, but that R-factor models that
349 specifically involve sulfide fractionation can explain the variations with reasonable amounts of
350 crustal assimilation (<1% to 4%). These models are so successful at explaining the variations in
351 coupled ^{186}Os-^{187}Os for layered intrusion chromitites that alternate explanations, such as core
352 interactions are simply not required in these circumstances. There is strong evidence from
353 $^{187}Os/^{188}Os$ data in many layered intrusions that incorporation of a crustal component is an
354 important, possibly ubiquitous, trigger for chromitite petrogenesis (e.g., Schoenberg et al. 1999;
355 Horan et al. 2001; Marques et al., 2003; Day et al., 2008; O'Driscoll et al. 2009), strongly
356 supporting the R-factor mixing models presented here. Whether the crustal component is
357 introduced by the mixing between crustal and mantle melts (cf. Irvine, 1977), or by assimilation
358 of footwall feldspathic cumulate (O'Driscoll et al., 2010), for which prior magma-crust

interactions may have been involved (so that crustal isotopic signatures can be 'recycled' in the magma reservoir), does not mitigate against these arguments.

4.5 Core-mantle interaction is not required to explain radiogenic ^{186}Os

A critical aspect of the new results for the Stillwater, Muskox and Rum layered intrusions is that significant $^{186}Os/^{188}Os$ variations occur within and between units that can only be explained by shallow crustal-level processes. Therefore, while deep mantle plume sources may have been postulated for some of these locations (e.g., Schaefer et al., 2000), they are not necessary to explain the radiogenic $^{186}Os/^{188}Os$ variations. For example, the Paleogene North Atlantic Igneous Province encompasses the Rum Layered Suite, as well as basaltic-picritic lavas occurring on Baffin Island, West Greenland, East Greenland, Ireland and the UK that are ancestral to modern-day Iceland. The new $^{186}Os/^{188}Os$ ratio for the West Greenland Fe-bearing cumulate is consistent with a primitive mantle-like composition, and no evidence for enriched ^{186}Os sources, similar to Icelandic lavas (Brandon et al., 2007). This is despite extensive interaction between carbonaceous sediment and basalt at the West Greenland locality (Pernet-Fisher et al., 2017), suggesting that enhanced enrichment of radiogenic ^{186}Os from crustal sources was not accomplished in an R-factor like model as proposed for chromitites. Compared with the Rum intrusion rocks, these results illustrate the importance of crustal contamination to generate ^{186}Os variations, without the need for deep mantle ^{186}Os enrichments. As with the example of Rum, the Muskox and Stillwater chromitite data are consistent with crustal contributions leading to $^{186}Os/^{188}Os$ ratios higher than primitive mantle compositions. In turn, these suggest that the Noril'sk $^{186}Os/^{188}Os$ ratios can also be explained by crustal contamination processes (**Figure 6**); indeed, extensive crustal contamination has been invoked at Noril'sk in order to explain the large sulfide ore deposits there (Barnes et al. 2017, and references therein).

To date, the only location where radiogenic $^{186}Os/^{188}Os$ has been measured in OIB is Hualalai on Hawaii (Brandon et al., 1999; Ireland et al., 2007). Radiogenic $^{186}Os/^{188}Os$ has also been measured in some (Kostomuska, Weltevreden, Gorgona) but not all (Komati, Abitibi, Belinge) komatiites (Brandon et al., 2003; Puchtel et al., 2005; 2014). Processes of minor continental crustal contamination are possible to envisage in some komatiites (e.g., Foster et al., 1996), but less so in Hawaiian basalts. For komatiites, high-temperatures of eruption have been shown to

lead to effective scavenging of the HSE by S-rich crustal contaminants. For Hawaiian basalts, no such sources are evident, with the underlying Pacific lithosphere considered to be relatively young (<90 Ma). Alternative sources of high Pt/Os are required for this location but might include enrichment from ancient high Pt/Os recycled oceanic crust contained within the peridotite mantle (O'Driscoll et al., 2015).

5. Conclusions

We have examined chromitites and peridotites from three mafic-ultramafic layered intrusions, as well as a native-Fe cumulate from West Greenland, and report significant variations in both measured and initial $^{186}Os/^{188}Os$ ratios. The lowest $^{186}Os/^{188}Os$ (0.119832) occurs in the West Greenland native iron cumulate, which is broadly consistent with data for Icelandic picrites (Brandon et al., 2007). In contrast, the ranges in $^{186}Os/^{188}Os$ for the ~2.7 Ga Stillwater (0.119838-0.119850), ~1.27 Ga Muskox (0.119847-0.119924) and ~0.06 Ga Rum (0.119842-0.119856) intrusions are large and track with $^{187}Os/^{188}Os$ variations in the same samples. We argue that this can only be explained by shallow-level mixing processes and crustal contamination. The highly siderophile element (HSE: Os, Ir, Ru, Pt, Pd, Re) contents of the chromitites and peridotites can be modelled through high sulfide-melt partitioning (typically >8000) illustrating the role of S-saturation and HSE scavenging. Taking both high sulfide-melt partitioning and high silicate melt-to-sulfide melt ratios (R-factor) into consideration, it is possible to successfully explain the variations in ^{186}Os-^{187}Os in layered intrusions using calculated Os isotope crustal evolution growth models. These calculations indicate that <4% of ancient high Pt/Os crustal contributions can explain the composition of the chromitites and peridotites that were examined, if effective sulfide scavenging of the HSE occurred. Our observations support models for chromitite genesis that invoke either crustal melt-primitive melt mixing (Irvine, 1977), or cumulate assimilation (O'Driscoll et al., 2010). The new data for layered intrusions also indicate that contamination by ancient high Pt/Os crustal materials can generate significant $^{186}Os/^{188}Os$ variations. This may be a possible reason for $^{186}Os/^{188}Os$ variations observed in some komatiites. It is more difficult to explain radiogenic $^{186}Os/^{188}Os$ measured in Hawaiian lavas by crustal contamination processes. Instead, ancient high Pt/Os ocean crust, shallow mantle sources that contain metasomatic sulfide, or metal-rich large low-shear wave velocity provinces at the core-mantle boundary all remain valid explanations.

Acknowledgements

We thank Paul Hollick and the Stillwater Mining Company for access to the Mountain View Section, Larry Hulbert for the Muskox chromitite samples, and Cyrena Goodrich for the West Greenland Native Fe sample.

References

Baker, J.A., Jensen, K.K., 2004. Coupled ^{186}Os–^{187}Os enrichments in the Earth's mantle–core–mantle interaction or recycling of ferromanganese crusts and nodules? *Earth and Planetary Science Letters*, 220, 277-286.

Barnes, S.J., Ripley, E.M., 2016. Highly siderophile and strongly chalcophile elements in magmatic ore deposits. *Reviews in Mineralogy and Geochemistry*, 81, 725-774.

Barnes, S.J., Holwell, D.A., Le Vaillant, M. 2017. Magmatic sulfide ore deposits. *Elements*, 13, 89-95.

Biggin, A.J., Piispa, E.J., Pesonen, L.J., Holme, R., Paterson, G.A., Veikkolainen, T., Tauxe, L. 2015. Palaeomagnetic field intensity variations suggest Mesoproterozoic inner-core nucleation. *Nature*, 526, 245-248.

Boudreau, A.E., 2016. The Stillwater Complex, Montana–Overview and the significance of volatiles. *Mineralogical Magazine*, 80, 585-637.

Brandon, A.D., Walker, R.J., Morgan, J.W., Norman, M.D. and Prichard, H.M., 1998. Coupled ^{186}Os and ^{187}Os evidence for core-mantle interaction. *Science*, 280, 1570-1573.

Brandon, A.D., Norman, M.D., Walker, R.J., Morgan, J.W., 1999. ^{186}Os-^{187}Os systematics of Hawaiian picrites. *Earth and Planetary Science Letters*, 174, 25-42.

Brandon, A.D., Snow, J.E., Walker, R.J., Morgan, J.W., Mock, T.D., 2000. ^{190}Pt-^{186}Os and ^{187}Re-^{187}Os systematics of abyssal peridotites. *Earth and Planetary Science Letters*, 177, 319-335.

Brandon, A.D., Walker, R.J., Puchtel, I.S., Becker, H., Humayun, M., Revillon, S., 2003. ^{186}Os–^{187}Os systematics of Gorgona Island komatiites: implications for early growth of the inner core. *Earth and Planetary Science Letters*, 206, 411-426.

Brandon, A.D., Walker, R.J., Puchtel, I.S., 2006. Platinum-osmium isotope evolution of the Earth's mantle: constraints from chondrites and Os-rich alloys. *Geochimica et Cosmochimica Acta*, 70, 2093-2103.

Brandon, A.D., Graham, D.W., Waight, T., Gautason, B., 2007. ^{186}Os and ^{187}Os enrichments and high-^{3}He/^{4}He sources in the Earth's mantle: evidence from Icelandic picrites. *Geochimica et Cosmochimica Acta*, 71, 4570-4591.

Campbell I.H., Naldrett A.J., 1979. The influence of silicate/sulphide ratios on the geochemistry of magmatic sulphides. *Economic Geology*, 74, 1503-1505.

Chatterjee, R., Lassiter, J.C., 2016. $^{186}Os/^{188}Os$ variations in upper mantle peridotites: constraints on the Pt/Os ratio of primitive upper mantle, and implications for late veneer accretion and mantle mixing trajectories. *Chemical Geology*, 442, 11-22.

Chazey, W.J., Neal, C.R., 2005. Platinum-group element constraints on source composition and magma evolution of the Kerguelen Plateau using basalts from ODP Leg 183. *Geochimica et Cosmochimica Acta*, 69, 4685-4701.

Coggon, J.A., Nowell, G.M., Pearson, D.G., Oberthür, T., Lorand, J.P., Melcher, F., Parman, S.W., 2012. The $^{190}Pt–^{186}Os$ decay system applied to dating platinum-group element mineralization of the Bushveld Complex, South Africa. *Chemical Geology*, 302, 48-60.

Cook, D.L., Walker, R.J., Horan, M.F., Wasson, J.T., Morgan, J.W., 2004. Pt-Re-Os systematics of group IIAB and IIIAB iron meteorites 1. *Geochimica et Cosmochimica Acta*, 68, 1413-1431.

Day, J.M.D., 2013. Hotspot volcanism and highly siderophile elements. *Chemical Geology*, 341, 50-74.

Day J.M.D., Pearson D.G., Hulbert L.J., 2008. Rhenium-osmium and platinum-group element constraints on the origin and evolution the 1.27Ga Muskox layered intrusion. *Journal of Petrology*, 49, 1255-1295.

Day, J.M.D., Pearson, D.G., Hulbert, L.J., 2013. Highly siderophile element behaviour during flood basalt genesis and evidence for melts from intrusive chromitite formation in the Mackenzie large igneous province. *Lithos*, 182, 242-258.

Day, J.M.D., Waters, C.L., Schaefer, B.F., Walker, R.J., Turner, S., 2016. Use of hydrofluoric acid desilicification in the determination of highly siderophile element abundances and Re-Pt-Os isotope systematics in mafic-ultramafic rocks. *Geostandards and Geoanalytical Research*, 40, 49-65.

Day, J.M.D., Brandon, A.D., Walker, R.J., 2016b. Highly siderophile elements in Earth, Mars, the Moon, and asteroids. Reviews in Mineralogy and Geochemistry, 81, 161-238.

Day, J.M.D., Walker R.J., Warren J.M., 2017. Os-186-Os-187 and highly siderophile element abundance systematics of the mantle revealed by abyssal peridotites and Os-rich alloys. *Geochimica et Cosmochimica Acta*, 200, 232-254.

Horan, M.F., Morgan, J.W., Walker, R.J., Cooper, R.W., 2001. Re–Os isotopic constraints on magma mixing in the peridotite zone of the Stillwater complex, Montana, USA. *Contributions to Mineralogy and Petrology*, 141, 446-457.

Humayun, M., 2011. A model for osmium isotopic evolution of metallic solids at the core-mantle boundary. *Geochem. Geophys. Geosys.* 12, Q03007, doi:10.1029/2010GC003281.

Ireland, T.J., Walker, R.J., Brandon, A.D., 2011. ^{186}Os-^{187}Os systematics of Hawaiian picrites revisited: New insights into Os isotopic variations in ocean island basalts. *Geochimica et Cosmochimica Acta*, 75, 4456-4475.

Irvine T.N., 1977. Origin of chromitite layers in the Muskox intrusion and other stratiform intrusions: A new interpretation. *Geology*, 5, 273-277.

Labrosse, S., Poirier, J.P., Le Mouel, J.L., 2001. The age of the inner core. *Earth and Planetary Science Letters*, 190, 111-123.

Lambert D.D., Walker R.J., Morgan J.W., Shirey S.B., Carlson R.W., Zientek M.L., Lipin B.R., Koski M.S., Cooper R.L., 1994. Re-Os and Sm-Nd isotope geochemistry of the Stillwater Complex, Montana: Implications for the petrogenesis of the J-M Reef. *Journal of Petrology*, 35, 1717-1753.

Lassiter, J.C., 2006. Constraints on the coupled thermal evolution of the Earth's core and mantle, the age of the inner core, and the origin of the ^{186}Os/^{188}Os "core signal" in plume-derived lavas. *Earth and Planetary Science Letters*, 250, 306-317.

Lassiter, J.C., Byerly, B.L., Snow, J.E., Hellebrand, E., 2014. Constraints from Os-isotope variations on the origin of Lena Trough abyssal peridotites and implications for the composition and evolution of the depleted upper mantle. *Earth and Planetary Science Letters*, 403, 178-187.

Luguet, A., Pearson, D.G., Nowell, G.M., Dreher, S.T., Coggon, J.A., Spetsius, Z.V., Parman, S.W., 2008. Enriched Pt-Re-Os isotope systematics in plume lavas explained by metasomatic sulfides. *Science* 319, 453-456.

Marcantonio, F., Zindler, A., Reisberg, L., Mathez, E.A., 1993. Re-Os isotopic systematics in chromitites from the Stillwater Complex, Montana, USA. *Geochimica et Cosmochimica Acta*, 57, 4029-4037.

Marques, J.C., Ferreira Filho, C.F., Carlson, R.W., Pimental, M.M. 2003. Re-Os and Sm-Nd isotope and trace element constraints on the origin of the chromitite deposit of the Ipueira-Medrado Sill, Bahia, Brazil. *Journal of Petrology*, 44, 659-678.

Meisel, T., Walker, R.J., Irving, A.J., Lorand, J.P., 2001. Osmium isotopic compositions of mantle xenoliths: a global perspective. *Geochimica et Cosmochimica Acta*, 65, 1311-1323.

Morgan J.W., Walker R.J., Horan M.F., Beary E.S., Naldrett A.J., 2002. ^{190}Pt-^{186}Os and ^{187}Re-^{187}Os systematics of the Sudbury Igneous Complex, Ontario. *Geochimica et Cosmochimica Acta*, 66, 273-290.

Mungall, J.E., Brenan, J.M., 2014. Partitioning of platinum-group elements and Au between sulfide liquid and basalt and the origins of mantle-crust fractionation of the chalcophile elements. *Geochimica et Cosmochimica Acta*, 125, 265-289.

Nimmo, F., 2007. Energetics of the core. *Treatise on Geophysics*, 8, pp.31-65.

O'Driscoll B., Day J.M.D., Daly J.S., Walker R.J., McDonough W.F. (2009) Rhenium-osmium isotope and platinum-group elements in the Rum Layered Suite, Scotland: Implications for Cr-spinel seam formation and the composition of the Iceland mantle anomaly. *Earth and Planetary Science Letters*, 286, 41-51.

O'Driscoll, B., Emeleus, C.H., Donaldson, C.H., Daly, J.S., 2010. Cr-spinel seam petrogenesis in the Rum Layered Suite, NW Scotland: cumulate assimilation and in situ crystallization in a deforming crystal mush. *Journal of Petrology*, 51, 1171-1201.

O'Driscoll, B., Walker, R.J., Day, J.M.D., Ash, R.D., Daly, J.S. 2015. Generations of melt extraction, melt-rock interaction and high-temperature metasomatism preserved in peridotites of the ~497 Ma Leka Ophiolite Complex, Norway. *Journal of Petrology*, 56, 1797-1828.

Pernet-Fisher, J.F., Day, J.M.D., Howarth, G.H., Ryabov, V.V., Taylor, L.A. 2017, Atmospheric outgassing and native-iron formation during carbonaceous sediment-basalt melt interactions. *Earth and Planetary Science Letters*, 460, 201-212.

Peucker-Ehrenbrink, B., Jahn, B.M., 2001. Rhenium-osmium isotope systematics and platinum group element concentrations: Loess and the upper continental crust. *Geochemistry, Geophysics, Geosystems*, 2(10).

Puchtel, I.S., Brandon, A.D., Humayun, M., Walker, R.J., 2005. Evidence for the early differentiation of the core from Pt–Re–Os isotope systematics of 2.8-Ga komatiites. *Earth and Planetary Science Letters*, 237, 118-134.

Puchtel, I.S., Walker, R.J., Touboul, M., Nisbet, E.G., Byerly, G.R., 2014. Insights into early Earth from the Pt–Re–Os isotope and highly siderophile element abundance systematics of Barberton komatiites. *Geochimica et Cosmochimica Acta*, 125, 394-413.

Schaefer, B.F., Parkinson, I.J., Hawkesworth, C.J., 2000. Deep mantle plume osmium isotope signature from West Greenland Tertiary picrites. *Earth and Planetary Science Letters*, 175, 105-118.

Schoenberg, R., Kruger, F.J., Nagler, T.F., Meisel, T., Kramers, J.D., 1999. PGE enrichment in chromitite layers and the Merensky Reef of the Bushveld complex; a Re–Os and Rb–Sr isotope study. *Earth and Planetary Science Letters*, 172, 49–64.

Upton, B.G.J., Skovgaard, A.C., McClurg, J., Kirstein, L., Cheadle, M., Emeleus, C.H., Wadsworth, W.J., Fallick, A.E., 2002. Picritic magmas and the Rum ultramafic complex, Scotland. *Geological Magazine*, 139, 437-452.

Walker, R.J., Morgan, J.W., Beary, E., Smoliar, M.I., Czamanske, G.K., Horan, M.F., 1997. Applications of the ^{190}Pt-^{186}Os isotope system to geochemistry and cosmochemistry. *Geochimica et Cosmochimica Acta*, 61, 4799-4808.

Walker, R.J., Brandon, A.D., Bird, J.M., Piccolli, P.M., McDonough, W.F., Ash, R.D., 2005. ^{187}Os-^{186}Os systematics of Os-Ir-Ru alloy grains from southwestern Oregon. *Earth and Planetary Science Letters*, 230, 211-226.

Figures and Figure Captions

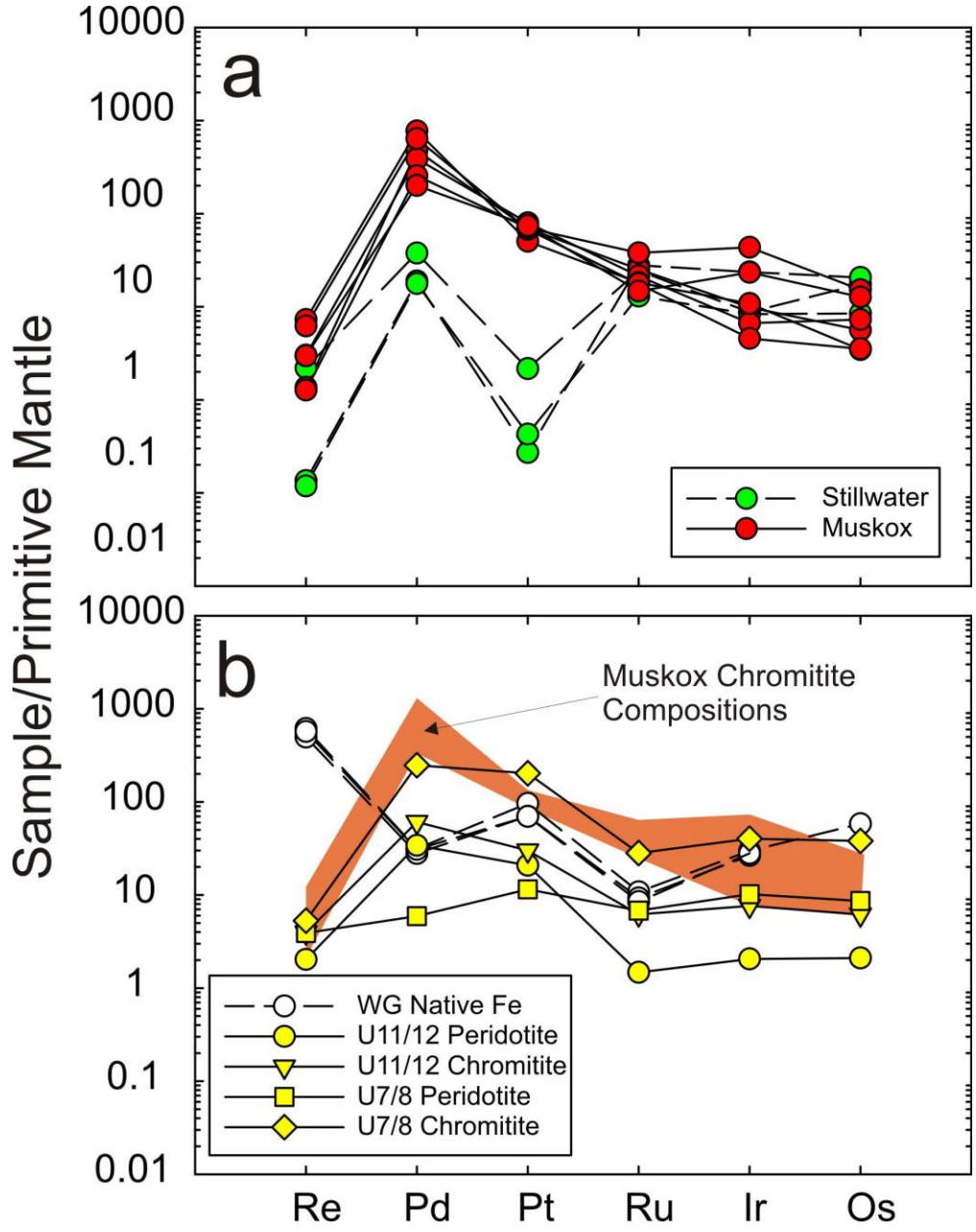

Figure 1: Primitive mantle normalized highly siderophile element patterns for (a) the Stillwater Igneous Complex and Muskox Intrusion chromitite samples, and (b) Rum Layered Suite peridotite and chromitite samples and the native iron bearing West Greenland sample (WG Native Fe). Primitive mantle normalization is from Day et al. (2017) and error bars are smaller than symbols.

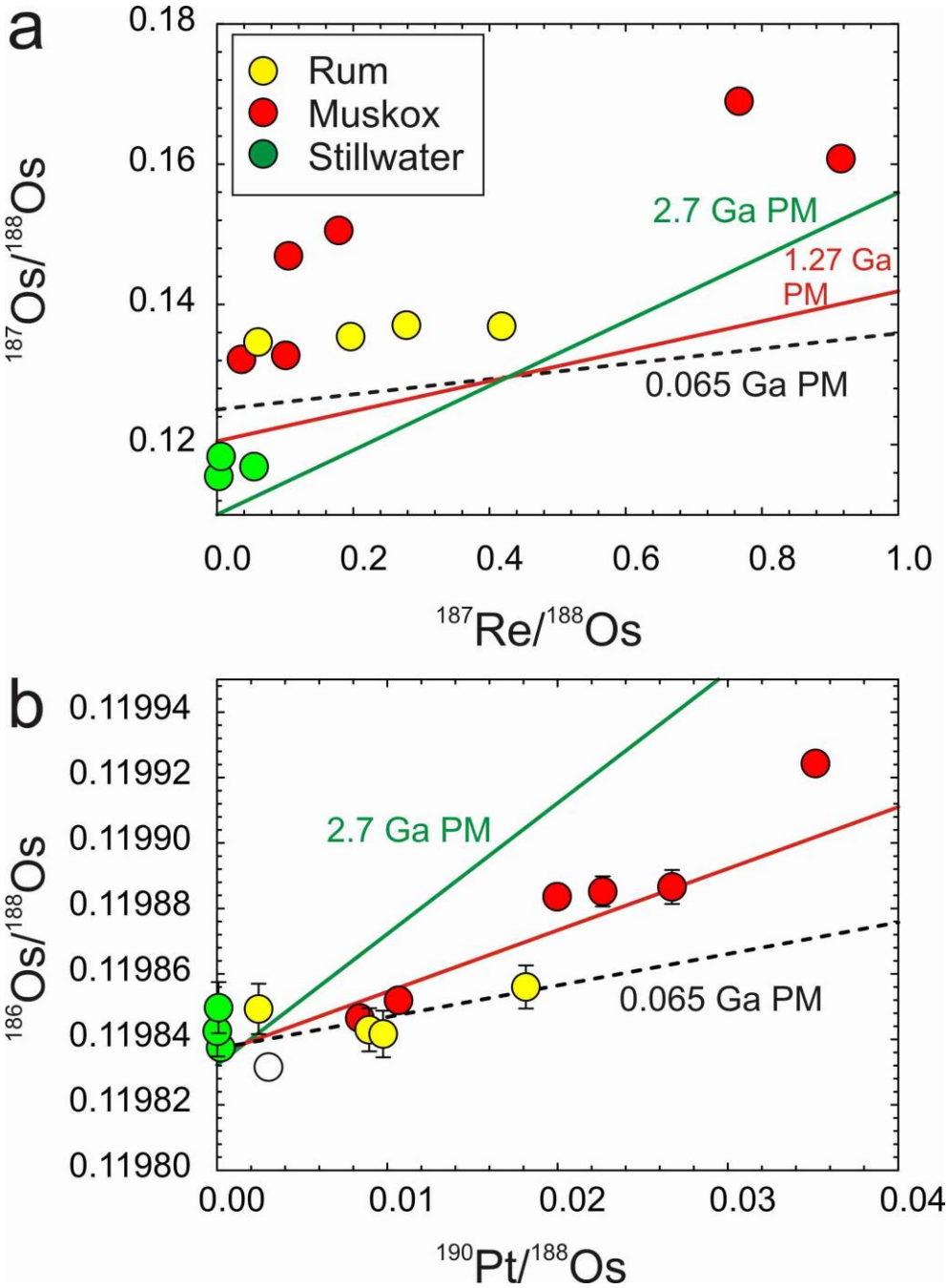

Figure 2: Plots of (a) $^{187}Re/^{188}Os$ versus $^{187}Os/^{188}Os$ and (b) $^{190}Pt/^{188}Os$ versus $^{186}Os/^{188}Os$ for Stillwater Igneous Complex and Muskox Intrusion chromitite samples and Rum Igneous Complex peridotite and chromitite samples. Shown are 2.7, 1.27 and 0.065 Ga reference isochrons for the two isotope systems, anchored to the primitive mantle $^{187}Os/^{188}Os$ and $^{186}Os/^{188}Os$ at that time. Error bars are shown, or are smaller than symbols.

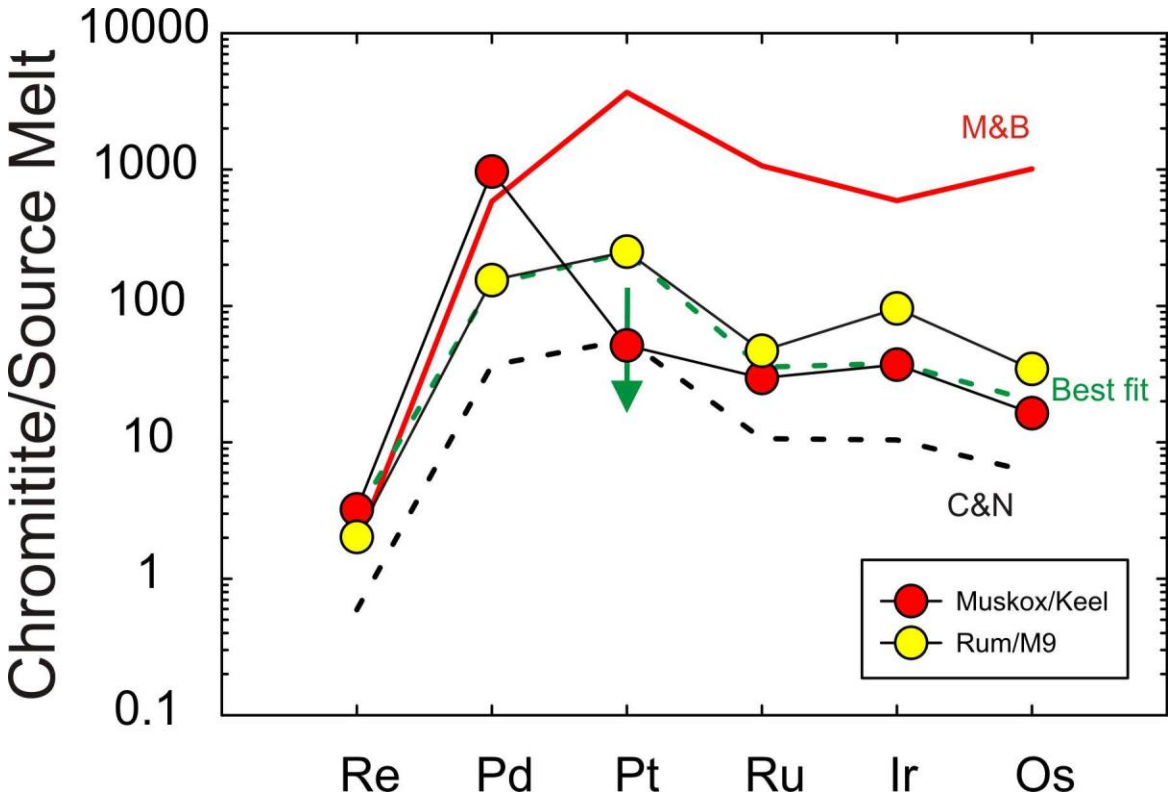

Figure 3: Enrichment factors for the average Muskox and Rum chromitite composition estimated by comparison with putative melt compositions from associated dikes. Models are for instant sulfide compositions during melt fractionation using the sulfide-melt partitioning from Mungall & Brenan (2014) [M&B] anchoring values to Pd sulfide-melt partitioning of 100,000 (Os = 400,000; Ir = 250,000; Ru = 240,000; Pt = 450,000; Re = 300) and the sulfide-melt partitioning estimated by Chazey & Neal (2005) assuming identical partition coefficients for Ru and Os (Ir = 4400, Ru, = 2400, Pt = 6900, Pd = 6300) and Re of 100. A best-fit model (green dashed line) to achieve the enrichments has sulfide-melt partitioning for Re of ~500, Os and Ru of ~8000, ~16,000 for Ir, ~25,000 for Pd and ~30,000 for Pt. The green arrow shows the effect of lower sulfide-melt partitioning to achieve the low Pt Stillwater chromitite compositions (~2000). The Muskox Keel dike and Rum M9 picrite dike compositions are from Day et al. (2008) and O'Driscoll et al. (2009), respectively.

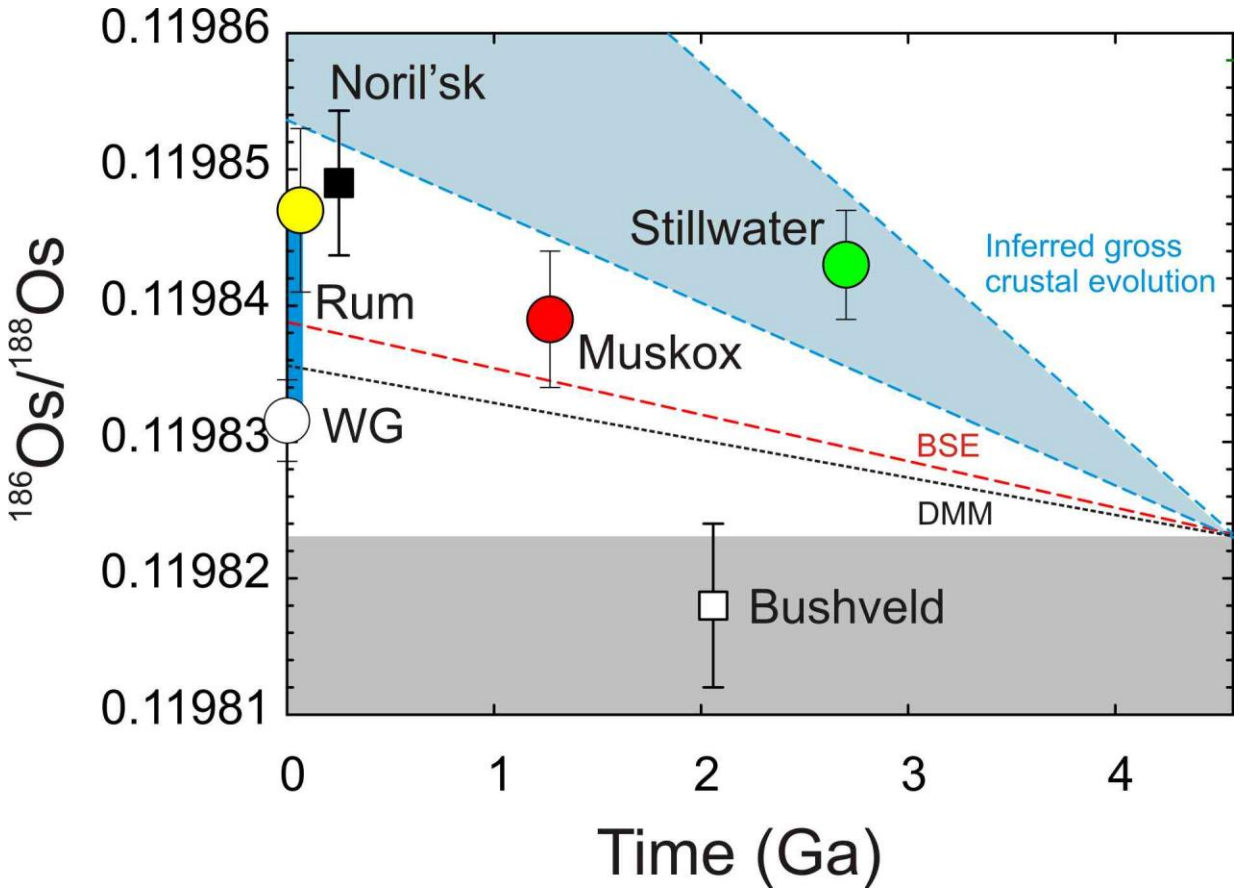

Figure 4: Platinum-osmium isotope evolution diagram for chromitite seam average compositions from the Stillwater Igneous Complex, Muskox Intrusion, Rum Layered Suite, a native Fe-bearing West Greenland sample, the Bushveld Igneous Complex (attained by LA-MC-ICP-MS; Coggan et al., 2011) and the Noril'sk Complex (Walker et al., 1997) with Pt/Os evolution curves for the DMM and BSE, as well as inferred gross crust and upper crust composition (this study and Peucker-Enrinkbrink & Jahn, 2001). Blue bar shows the range in $^{186}Os/^{188}Os$ measured for modern terrestrial basalts (Brandon et al., 2007; Ireland et al., 2011). Grey shaded region denotes area below the Solar System Initial value (see Day et al., 2016b). Evolution curves for DMM and BSE are from Day et al. (2017).

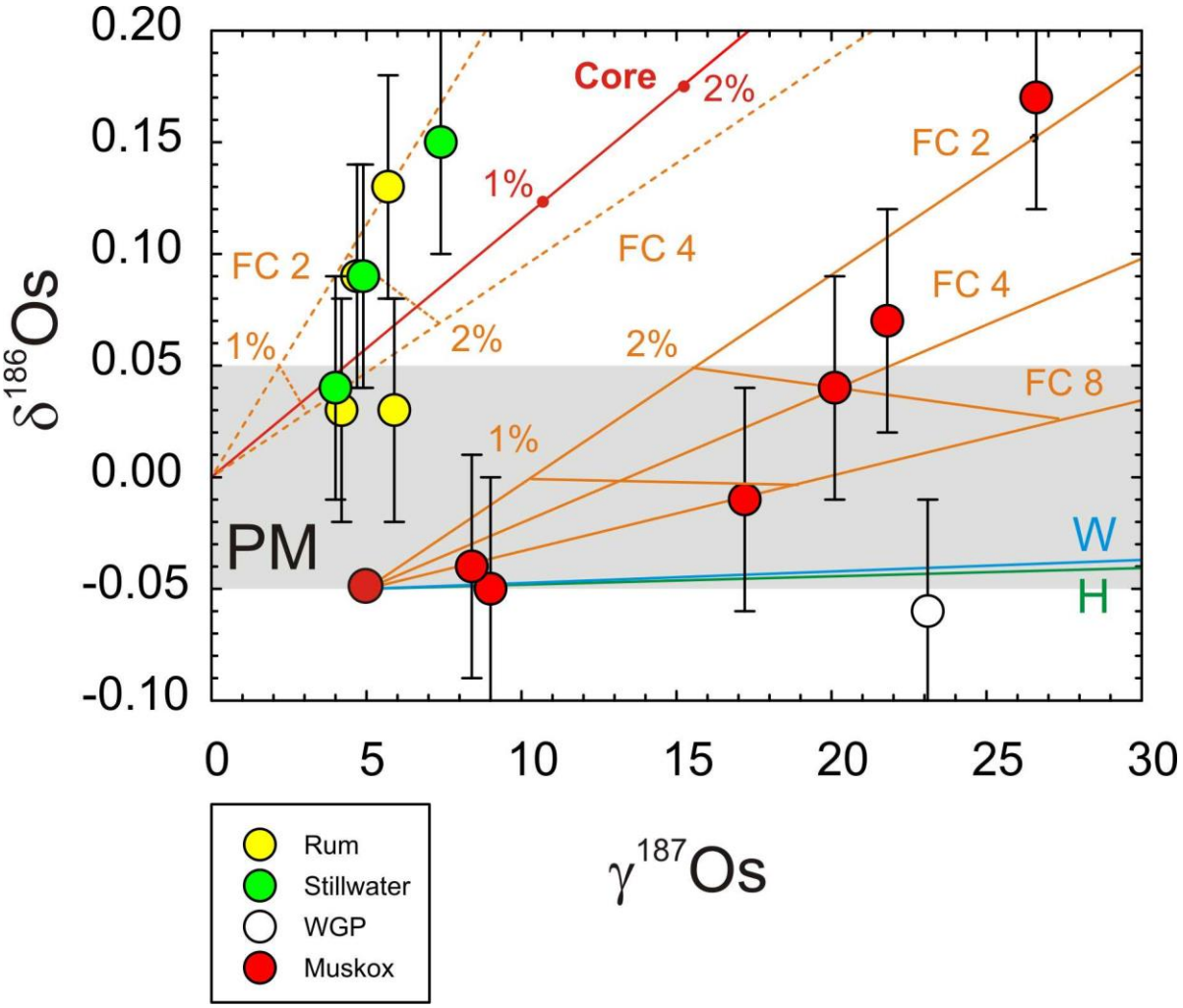

Figure 5: Models of osmium isotopic compositions resulting from core additions and crustal contributions to primitive mantle melts (Gray field of error for PM composition). Shown is a core addition model using values from Brandon et al. (2003) (Red line) and models for >1.8 Ga Wopmay Paragneiss (W) and 1.66 Ga Hornby Bay Sandstone (H) contamination in a Muskox Keel dike composition from Day et al. (2008). Orange dashed lines show models of mixing between PM and calculated crustal sources involving an R-factor model (1000:1) after fractional crystallization and sulfide fractionation (see text for details). Orange solid lines denote the mixing models, but with a source composition with low δ^{186}Os (-0.05) and higher γ^{187}Os (+5), as inferred for the Muskox Intrusion. Model curves shown with percentage increments.

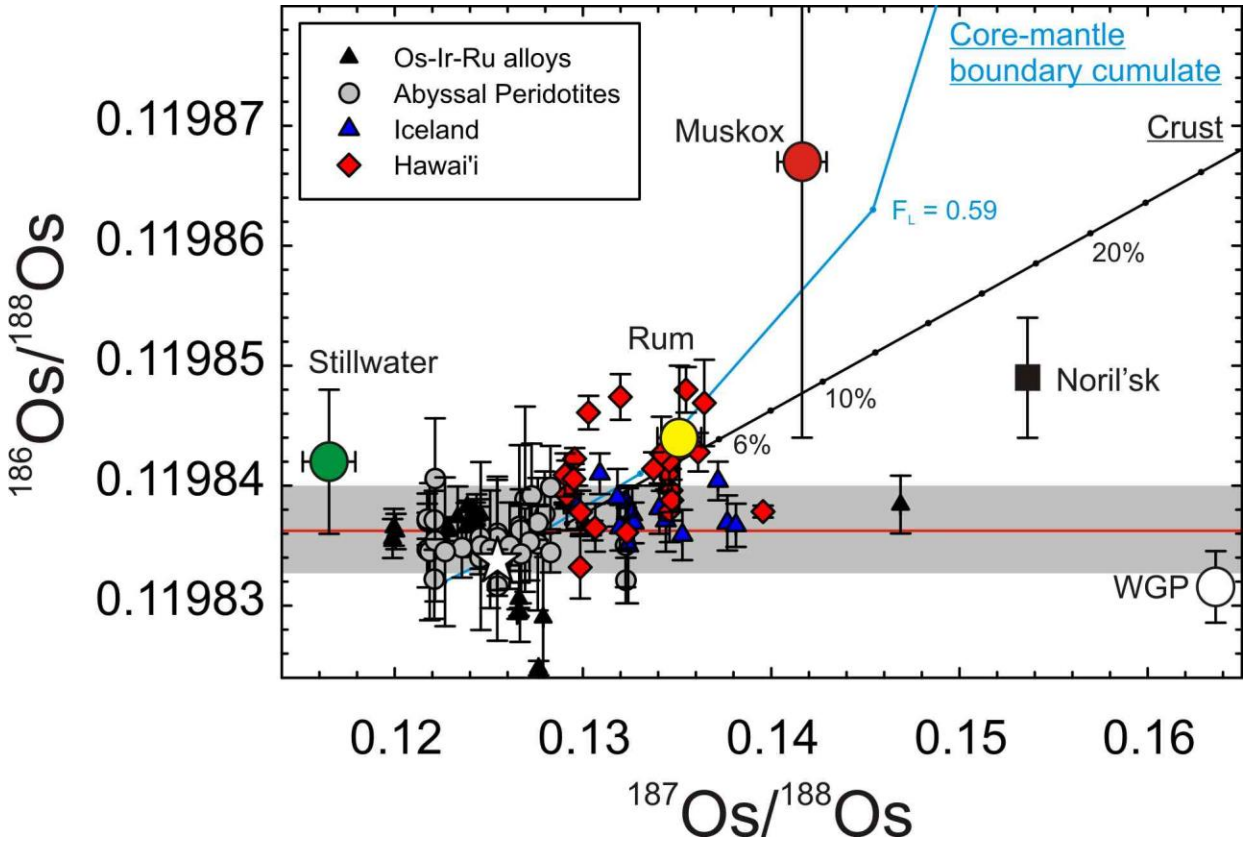

Figure 6: Osmium isotope systematics of layered intrusions average compositions versus abyssal peridotite compositions, Os-rich alloys, and lavas from Iceland and Hawai'i with the composition of the carbonaceous chondrite Allende provided for comparison (star). Shown are a core-mantle boundary cumulate model from Humayun (2011) and a crustal contamination model (FC4) from Figure 5. Data for abyssal peridotites, Os-rich alloys and Allende are from Brandon et al. (2000), Chaterjee & Lassiter (2016) and Day et al. (2017b), respectively. Data for Hawaiian lavas are from Ireland et al. (2011) and for Icelandic lavas are from Brandon et al. (2007).

Table 1: Highly siderophile element abundances and ^{187}Os-^{186}Os systematics for layered intrusions

Sample	Horizon	Re	Pd	Pt	Ru	Ir	Os	$^{187}Re/^{188}Os$	2SE	$^{190}Pt/^{188}Os$	2SE	$^{187}Os/^{188}Os$	2SE	$^{186}Os/^{188}Os$	2SE	$\gamma Os_{(PM)}$	$\delta Os_{(PM)}$
2.7 Ga Stillwater Intrusion, USA																	
ST1203	G	0.77	199.56	16.23	192.52	31.40	67.78	0.05460	0.00082	0.000227	0.000003	0.116859	0.000003	0.1198375	0.0000033	4.0	0.04
ST1204	G	0.05	99.89	2.04	220.48	84.78	80.35	0.002841	0.000043	0.000024	0.000000	0.115473	0.000008	0.1198425	0.0000077	4.9	0.09
ST1217A	H	0.04	94.00	3.21	102.73	30.00	33.03	0.006062	0.000091	0.000092	0.000001	0.118337	0.000007	0.1198497	0.0000078	7.4	0.15
1.27 Ga Muskox Intrusion, Canada																	
HDB-2000-MX4a	Unit 22	0.475	2524.9	520.18	199.82	35.449	21.86	0.1050	0.0016	0.022650	0.000340	0.146942	0.000005	0.1198852	0.0000046	20.1	0.04
		1.053	2054.5	597.56	168.77	24.038	28.48	0.1787	0.0027	0.019978	0.000300	0.150555	0.000003	0.1198836	0.0000024	21.8	0.07
HDB-2000-MX26a	Unit 22	2.550	4096.5	377.65	143.40	38.920	13.48	0.916	0.014	0.026719	0.000401	0.160788	0.000005	0.1198866	0.0000052	17.2	-0.01
		2.174	3379.7	506.03	139.59	16.430	13.74	0.766	0.011	0.035147	0.000527	0.168992	0.000003	0.1199243	0.0000027	26.6	0.17
HDB-2000-MX40a	Unit 22	0.444	1354.9	524.39	299.66	156.52	59.34	0.0361	0.0005	0.008395	0.000126	0.132171	0.000002	0.1198465	0.0000014	9.0	-0.05
		1.038	1065.0	557.28	116.10	84.345	49.65	0.1008	0.0015	0.010664	0.000160	0.132730	0.000001	0.1198519	0.0000009	8.4	-0.04
0.060 Ga Rum Intrusion, UK																	
Unit 12 Peridotite	Unit 11/12	0.710	180.90	156.40	11.64	7.41	8.20	0.4180	0.0063	0.018137	0.000272	0.136896	0.000006	0.1198560	0.0000066	5.7	0.13
Unit 11/12 Chromitite	Unit 11/12	1.383	322.84	225.60	48.81	27.48	24.00	0.2781	0.0042	0.008934	0.000134	0.137031	0.000006	0.1198429	0.0000066	5.9	0.03
Unit 8 Peridotite	Unit 7/8	1.366	31.45	86.28	53.62	36.74	33.60	0.1961	0.0029	0.002440	0.000037	0.135412	0.000009	0.1198493	0.0000077	4.7	0.09
Unit 7/8 Chromitite	Unit 7/8	1.852	1311.86	1524.69	222.86	144.87	148.42	0.0602	0.0009	0.009762	0.000146	0.134641	0.000008	0.1198416	0.0000071	4.2	0.02
0.06 Ga West Greenland Native Iron Cumulate																	
WGLB	Disko Island	214.7	166.1	719.8	85.4	106.6	226.7	4.59	0.07	0.003028	0.000045	0.1636055	0.0000029	0.1198316	0.0000030	23.1	-0.06
		173.5	147.7	524.0	73.2	95.3											
		199.9	163.4	522.8	66.9	100.9											